

PFC/JA-96-24

**Negative Magnetic Shear Modes of Operation in
the Alcator C-Mod Tokamak Near the Beta Limit**

P.T. Bonoli, M. Porkolab, J.J. Ramos, W. Nevins¹, C. Kessel²

June, 1996

¹Lawrence Livermore National Laboratory, Livermore, CA.

²Princeton Plasma Physics Laboratory, Princeton, NJ.

Plasma Physics and Controlled Fusion.

This work was supported by the U. S. Department of Energy Contract No. DE-AC02-78ET51013. Reproduction, translation, publication, use and disposal, in whole or in part by or for the United States government is permitted.

**Negative Magnetic Shear Modes of Operation
in the Alcator C-Mod Tokamak Near the Beta Limit**

P.T. Bonoli, M. Porkolab and J.J. Ramos,

Plasma Fusion Center

Massachusetts Institute of Technology

Cambridge, MA 02139

W. Nevins

Lawrence Livermore National Laboratory

Livermore, CA 95540

C. Kessel

Plasma Physics Laboratory

Princeton University

Princeton, NJ 08543

Abstract

The stability properties of non-inductively driven, reversed shear type current profiles that may be achieved for Alcator C-Mod tokamak-like parameters (aspect ratio $R/a=3$) are examined. It is found that without a conducting wall, the best stability results (β_N up to 3.7) are achieved for highly triangular plasmas ($\delta = 0.7$) at $q_{\min}=2.2$, for relatively broad pressure profiles ($p(0)/p_{\text{avg}} = 2.8$) and large values of $r_{\min}/a (= 0.75)$. For elliptical or circular cross-section plasmas with little triangularity, the stability limits are significantly lower ($\beta_{N\text{max}}=2.2$). Finally, more peaked pressure profiles ($p(0)/p_{\text{avg}} = 4.5$) have lower beta limits than broader profiles.

I. Introduction

Demonstrating the feasibility of tokamak operation in steady state with relatively high values of β_N , high confinement and high bootstrap current fraction is becoming increasingly more important for a commercially attractive fusion reactor concept[1]. Recent predictions of highly improved tokamak performance in the presence of negative (or reversed) magnetic shear[2,3] have generated great interest in understanding the beta limits of such equilibria. Moreover, recent experimental observations of greatly reduced transport in plasmas with negative central shear provide strong motivation to further explore techniques by which such equilibria may be established and maintained for time scales beyond the characteristic current diffusion time (or L/R time) [4,5]. We note that the recent experiments were transient in nature, and therefore a clear experimental verification, and theoretical understanding of the steady state properties and beta limits of negative central shear (NCS) discharges is still lacking. Important plasma properties which may influence the stability limits of negative central sheared plasma equilibria include pressure profile peaking and shaping (ellipticity and triangularity). The presence of a conducting shell and plasma rotation may also be important if high values of β_N (beyond four) are desired, or if we are dealing with relatively high aspect ratios (of the order of four or more, such as TPX [1]). Nevertheless, the exploration of stability limits for aspect ratios around $R/a=3$, such as Alcator C-Mod, is important not only for present day tokamaks, but also for exploring this mode of operation in ITER.

In the present work we shall summarize results of modeling studies of negative central shear equilibria in the Alcator C-Mod tokamak. Subsequent to establishing self-consistent equilibria and current drive scenarios using the ACCOME code, we carry out stability analysis utilizing the Pest-II stability code, and determine the beta limits for a range of equilibria, including a highly triangular, an elliptic, and a circular shaped plasma cross section. The target plasma is maintained by means of off-axis lower-hybrid current drive, central ICRF heating and a modest amount of central fast wave current drive. At plasma pressures that can be generated by reasonable amounts of RF power (4-6 MW total) with an H-factor of 2.5, significant bootstrap fraction (typically 0.75) can be generated in C-Mod. It is worth noting that in C-Mod pulse-lengths up to 7 sec. can be maintained with non-inductive current drive assist at $B_T \leq 5$ T. As we shall see, $\beta_N \simeq 3$ can be achieved

at parameters corresponding to a skin time of $\tau_s \simeq 1$ sec., $\tau_{L/R} \simeq 3$ sec., and hence $t_{\text{pulse}}/\tau_{L/R} \lesssim 2$. Hence reversed-shear scenarios under quasi-steady state conditions could be achieved in C-Mod. The plasma parameters used in the present studies are established most effectively by an EXCEL spreadsheet calculation described in Sect. II.

II. Current Profile Control Studies

A. Model Description

The starting point for our current profile control studies is the specification of a consistent set of plasma pressure and RF heating power. This is accomplished using the EXCEL spreadsheet “1/2-D”, where the electron and ion temperatures at the operating point are obtained from 0-D power balance, assuming that the confinement time is H times greater than that predicted by the ITER89P L-mode scaling law [6] (i.e., we assume an H-mode multiplier). However, the spreadsheet also supports specified profiles of the temperature and density, which are used in relating volume averages, line averages, and peak values of density, temperature, and pressure. Power balance is computed separately for electrons and ions, including ohmic heating, auxiliary heating (for RF heating the power is divided between electrons and ions as specified by the user, while for neutral beam heating the power partition between electrons and ions is computed following Mikkelsen and Singer[7]). In addition, bremsstrahlung and synchrotron radiation (following the ITER Physics Design Guidelines[6]) and the collisional transfer of energy between electrons and ions (using the classical energy exchange rate evaluated at the volume averaged density and the density-weighted, volume-averaged temperature) are also included. While not relevant to the Alcator C-Mod points described here, the EXCEL spreadsheet supports plasma self-heating due to D-T fusion reactions. The electron and ion density profiles are assumed to have the same shape. However, the ion density is generally less than the electron density due to fuel dilution by impurities (computed self-consistently from user-specified impurity concentrations). The temperature profiles are also assumed to have the same shape, but with different peak values to reflect the different average electron and ion temperatures as computed from 0-D power balance as described above. The user specifies the profile of the safety factor. For the reversed-shear modes considered here, the values of q at the magnetic axis (q_0), at the limiter or 95% flux surface (q_a), the minimum value of the safety factor

q_{\min} and the value of poloidal flux at which the minimum occurs (ψ_{\min}), are specified. The spread sheet computes the coefficients of a 4th order polynomial q-profile such that the associated current profile has vanishing current density at the plasma surface. The q-profile and current density are related to each other by requiring that, on each flux surface, the relation[6]

$$q(\psi) = \frac{5r^2 B_0}{R_0 I(\psi)} \left[\frac{1 + \kappa^2(1 + 2\delta^2 - 1.2\delta^3)}{2} \right] f(r/R_0)$$

holds, where $I(\psi)$ is the current enclosed by the flux surface, r is the minor radius of the flux surface, and

$$f(\varepsilon) \equiv \frac{1 + 0.62\varepsilon - 2.22\varepsilon^2}{(1 - \varepsilon^2)^2} .$$

The profile of the neoclassical bootstrap current is computed following Hirshman [8], with collisional corrections included following Harris[9]. A comparison between the profile of the total current and that of the bootstrap current provides us with an initial estimate of the magnitude and location of the current that must be provided by rf current drive. This code was used to provide the plasma parameters for the ACCOME code studies. This initial estimate is refined by iteration between detailed computations of the lower hybrid and fast wave driven currents and recomputations of the MHD equilibrium using the ACCOME code as described in the remainder of this section.

An important element in the MHD stability studies of advanced tokamaks is the computation of the required plasma current density profiles. The current profile control calculations are carried out using the ACCOME code [10,11]. This simulation model combines a free boundary solution of the Grad Shafranov equation in noncircular geometry [12], with the calculation of driven currents due to neutral beam injection [13], lower hybrid (LH) waves [14], injected ICRF fast waves [15], and bootstrap effects [13]. The equilibrium and current drive modules iterate between each other to obtain an MHD equilibrium which is consistent with the profiles of driven current density. The density, temperature, and pressure profiles are prescribed in ACCOME. The particular temperatures and densities used in these studies have been obtained for the Alcator C-Mod tokamak parameters using the EXCEL spreadsheet described above, the expected tokamak performance, and

the near future available RF power. The MHD equilibria and current density profiles from ACCOME are coupled to the JSOLVER/PEST [16,17] equilibrium and stability package. Thus the current profile control results from ACCOME can be tested for stability to the $n = \infty$ ballooning mode and the low $n=(1,2,3)$ external kink modes.

The LH current drive (LHCD) package [11,14] utilizes a toroidal ray tracing code and parallel velocity Fokker Planck calculation to compute the wave-induced quasilinear flux and the absorbed rf power density $S_{\text{rf}}(\psi)$. The rf flux is used in an adjoint solution [18] of the Fokker Planck equation to evaluate the LHRF current drive efficiency. The driven LH current density is obtained by taking the product of the rf power dissipation and the current drive efficiency. The fast wave current drive (FWCD) package [15] employs a full-wave ICRF code [19] to compute the FW power deposition and a parameterization [20] of the FWCD efficiency. The FW current density is also computed by taking the product of the current drive efficiency and the ICRF power deposition. The bootstrap current drive module evaluates the Hirshman- Sigmar [21] expressions for the bootstrap current density in the banana-plateau collisionality regime. Multiple ion species are included exactly by solving the parallel momentum balance equation for each ion species separately. Trapping effects on the bootstrap current density are included by an exact evaluation of the two-dimensional spatial integrals given in Ref. [21].

In Sects. IIB and IIC we describe a set of current profile control results that were obtained for a tokamak configuration typical of the Alcator C-Mod device [22]. In these studies, LH current drive is used for control of the off-axis current profile and fast wave current drive (FWCD) is used to control the central current density. The remaining current drive is provided by bootstrap effects.

B. Current Profile Control Results for Plasma Shaping Study

In Figs. (1-3) we show the current profile control results for three different plasma configurations on Alcator C-Mod. In all three cases $B_o = 4.0$ T, $a = 0.23$ m, $R_o = 0.665$ m, $p(\psi) = p(0)(1 - \psi)^2$, $T(\psi) = T(0)[\frac{2}{3}(1 - \psi)^{7/2} + \frac{1}{3}(1 - \psi^8)^{3/2}]$, $n(\psi) = p(\psi)/T(\psi)$, $n_e(0) = 2.0 \times 10^{20} \text{ m}^{-3}$, and the plasma gas is deuterium. In the highly shaped and elliptical configurations the temperatures were $T_e(0) = T_D(0) = 7.5$ keV. In the circular configuration it was assumed that $T_e(0) = T_D(0) = 5.0$ keV. The off-axis

current profile control is provided by 3.0 MW of LHRF power at 4.6 GHz and the central seed current density is provided by (0.15-0.65) MW of ICRF fast wave power at 40 MHz. The parallel refractive index of the LH waves was varied in the range $2.9 \leq n_{\parallel} \leq 3.55$ and the toroidal mode number of the ICRF waves was set at $n_{\phi} = 4$. Using the EXCEL spreadsheet we find that an additional ICRF heating power of 3–4 MW, with an H-factor of 2.5 at $I_p = 800$ kA is required to attain these plasma parameters in the shaped tokamak configuration. Interestingly, the typical skin time at such parameters is of the order of $\tau_S \simeq 1$ sec., so that $\tau_{\text{pulse}}/\tau_{L/R} \lesssim 2$, as mentioned in the Introduction.

The case shown in Fig. 1(a) represents the highly shaped configuration with $\kappa_{\chi} = 1.77$ and $\delta_{\chi} = 0.71$. The total plasma current is $I_p = 807$ kA with bootstrap current fraction $f_{BS} = 0.74$, $I_{LH} = 196$ kA, and $I_{FW} = 9$ kA. The profiles of the bootstrap current, lower hybrid current, central fast wave seed current and the total current are shown in Fig. 1(b). The central value of the safety factor is $q_0 = 3.95$ with $q_{\min} = 2.65$, $q_{95} = 6.35$, and internal inductance $\ell_i(3) = 0.65$. The radius of shear reversal in this case [Fig. 1(c)] is at a normalized square root of the toroidal flux of $\rho \approx 0.71$. The volume average toroidal beta is $\beta_t = 2.60\%$ with a pressure peaking factor of $p(0)/p_{\text{avg}} = 2.90$, where p_{avg} stands for the volume averaged pressure.. The normalized beta is $\beta_N = \beta_t/(I_p/aB_0) = 2.96$ (% – mT/MA). The central LH ray trajectories [$n_{\parallel}^{LH}(0) = 3.00$] incident from three poloidal launch points [$z_0 = (-0.1, 0, +0.1)$ m] are shown in Fig. 1(d). Each tick mark along the ray paths indicates a 10% decrease in the incident wave power due to quasilinear electron Landau damping. Complete single pass damping of the LHRF power is observed at these parameters in C-Mod.

The case shown in Fig. 2(a) is the elliptical plasma configuration where $\kappa_{\chi} = 1.86$ and $\delta_{\chi} = 0.10$. The plasma current is somewhat higher than in the previous case with $I_p = 952$ kA, $f_{BS} = 0.73$, $I_{LH} = 222$ kA, and $I_{FW} = 38$ kA. The current profile (Fig. 2(b)) and the profile of the safety factor (Fig. 2(c)) is similar to Fig. 1, with $q_0 = 3.96$, $q_{\min} = 2.57$, $q_{95} = 4.62$, and $\ell_i(3) = 0.65$. The shear reversal radius is $\rho \approx 0.72$. The lower value of q_{95} in this case is due to the higher current and to the fact that the separatrix is farther away from the plasma. In the elliptical plasma $\beta_t = 2.63\%$, $\beta_N = 2.54$, and $p(0)/p_{\text{avg}} = 2.87$.

The third case in the plasma shaping study is the circular plasma configuration shown in Fig. 3(a), where $\kappa_\chi = 1.00$ and $\delta_\chi = 0.07$. The current profile control results in this case are $I_p = 492$ kA, $f_{BS} = 0.73$, $I_{LH} = 120$ kA, $I_{FW} = 11$ kA, $q_0 = 3.45$, $q_{min} = 2.01$, $q_{95} = 3.98$, and $\ell_1(3) = 0.84$. The current profiles are shown in Fig. 3(b) and the safety factor profiles are shown in Fig. 3(c). The shear reversal radius remains at $\rho \approx 0.71$. The β_t and β_N are respectively 1.65% and 3.29. Due to the absence of plasma elongation in this case, the pressure peaking factor is only $p(0)/p_{avg} = 1.43$. The current density of this configuration must be scaled if q_0 and q_{min} are to be comparable to the previous two configurations. This implies a rescaling of the current and q_{95} by approximate factors of 0.873 and 1.140 respectively.

C. Current Profile Control Results for Peaked Pressure Profile

A relatively broad pressure profile was assumed for the studies in the previous Subsection. In this Subsection a more peaked pressure profile is used, which also contains a mild pedestal in the plasma periphery. Specifically, the form of the pressure was assumed to be $p(\psi) = p(0)[0.95(1-\psi)^4 + 0.05(1-\psi^6)^{3/2}]$. The temperature profile is identical to the form used in the previous Subsection and the density is $n(\psi) = p(\psi)/T(\psi)$. Other important parameters for this case are $n_e(0) = 1.4 \times 10^{20} \text{m}^{-3}$, $T_e(0) = T_D(0) = 10.7$ keV, $B_o = 4.0$ T, $P_{LH} = 1.5$ MW, $n_{\parallel}^{LH}(0) = 2.90$, $P_{FW} = 0.01$ MW, and $n_\phi = 4$. The electron density was lowered to improve the LH wave accessibility and thus allow wave penetration and current generation nearer the plasma center. This results in a decrease in the shear reversal radius. The decrease in shear reversal radius was desired in order to keep the minimum in safety factor at a point where the pressure gradient is large. The temperatures were increased in order to keep the central pressure comparable to the cases with broad pressure profiles. Due to the high electron temperature, complete single pass absorption of the lower hybrid waves occur.

The current profile control results for the peaked pressure profile are shown in Figs. 4(a) and 4(b). The plasma shape is similar to the highly shaped configuration shown in Fig. 1(a) with $\kappa_\chi = 1.78$ and $\delta_\chi = 0.71$. The total plasma current is $I_p = 811$ kA and the bootstrap current fraction is 0.56. The LH current drive is relatively large ($I_{LH} = 358$ kA) because of the low off-axis densities present at the location of LHRF power deposition. A

small seed current is provided by the fast wave with $I_{FW} = 1.8$ kA. The pressure peaking factor is now $p(0)/p_{avg} = 4.75$ and the plasma and normalized betas are 1.57% and 1.78 respectively. The q -profile is inverted with $q_0 = 2.72$, $q_{min} = 2.01$, $q_{95} = 5.77$, $\ell_i(3) = 0.86$, and the shear reversal radius has decreased to $\rho \approx 0.62$.

III. MHD Stability

Tokamak equilibria with the characteristics described in the previous section, i.e. reversed magnetic shear and relatively high minimum q , have attractive MHD stability properties. They are stable against $n = \infty$ ballooning modes, with easy global access to the second stability region. This allows high values of β_p with the associated high bootstrap current fraction. However, two kinds of instabilities unique to the double-valued safety factor profiles may arise, namely double tearing modes [23] and so called “infernal” modes [24,25]. In addition, like in every other tokamak configuration, one must maintain stability against low- n external modes.

Double tearing modes or other dissipative instabilities with two resonant surfaces on the double-valued q profile can have very low or zero beta thresholds, causing a disruptive termination of the plasma. The general rule to avoid these is to keep the minimum of q above 2.0 so that the dangerous large scale modes with m/n numbers 1/1, 3/2 and 2/1 do not have resonant surfaces. Any proposed operation at $q_{min} < 2$ should be carefully scrutinized because of the danger of double tearing or similarly induced disruptions.

The so called infernal modes are ideal MHD pressure driven modes that localize in the low shear region around the minimum of q . They are essentially internal (i.e. do not require a perturbation of the plasma boundary), can have intermediate or large mode numbers and are not accounted for by the conventional $n = \infty$ ballooning theory. Their danger stems from the fact that they can have very low beta limits, do not exhibit second stability regions, and manifest themselves in a multitude of mode numbers. The general prescription to avoid them is to avoid large pressure gradients coinciding with the zero shear point, and also to keep a relatively high q_{min} so as to have good average magnetic curvature since these modes are in some sense related to interchange modes.

In the present work we consider only equilibria with $q_{\min} > 2$ so that double tearing modes should not be an issue, and the stability analysis will be limited to the framework of ideal MHD. It will also be verified that the equilibria of the class described in the previous section which are the subject of our work, are not limited by “infernal” instabilities in the strict sense of such term [25]. The hard MHD limit is always found to be set by the $n=1$ external (pressure-current driven kink) mode, like in most other advanced tokamak configurations. However the Fourier structure of such mode in our reversed shear equilibria does exhibit features reminiscent of the double tearing and the infernal modes. Thus the poloidal harmonic with the first resonance in the plasma above q_{\min} has two marked singular layers and is dominant when nq_{\min} is close to an integer from below. The harmonic with the nearest resonance outside the plasma below q_{\min} has an interchange or “infernal” character, localized around the minimum of q , and is dominant when nq_{\min} is close to an integer from above. In addition the mode has significant external components with leading harmonics corresponding to the first resonances outside the plasma above $nq(a)$, like in the conventional external kinks.

These $n=1$ external modes are the main subject of our stability analysis. In this work, no conducting walls are assumed around the plasma, and the magnetic perturbation in the vacuum is allowed to extend to infinity. To carry out such stability analysis, the equilibria generated with the ACCOME code are recomputed on a finer grid of 200 flux surfaces and 256 poloidal points with the JSOLVER code, using as input the plasma boundary and the $p(\psi)$ and $\langle j_{\parallel} \rangle(\psi)$ profiles given numerically by the ACCOME solution. The JSOLVER equilibrium is then analyzed for low- n mode stability with the PEST-II code. A numerical convergence study of the PEST-II results is necessary. To this end, the radial (flux) resolution of each JSOLVER equilibrium is increased by interpolation according to a series of grids with geometrically increasing number of points. PEST-II eigenvalues are computed for each grid until a power-law dependence of the discretization error as a function of the grid size is established, which allows the extrapolation to the zero-mesh-size limit. Since the MHD limits depend only on dimensionless parameters, the results are applicable to any tokamak with the same aspect ratio, namely $A=2.9$, which makes them relevant not only to Alcator C-Mod but also to most other major tokamaks, such as TFTR, DIII-D, Ignitor and ITER. The results of our studies are displayed in Figs. 5-8.

We find that the two highly triangular equilibria obtained in the first and fourth cases of the previous section Figs.(1) and (4), are stable to all ideal MHD modes without conducting walls (see Figs. 5,8). The second (elliptical, Fig. 2) and third (circular, Fig. 3) cases are unstable to the $n=1$ external mode (Figs. 6 and 7 respectively). In order to obtain a better picture of the stability results, it is useful to generate a two-dimensional parameter space out of each ACCOME equilibrium, and to find there the marginal stability boundaries. To do that we scale by approximately overall multiplicative constants the pressure and current profiles of the ACCOME equilibria, thus spanning two-dimensional spaces with β_p and q_* axes. Such diagrams are shown in Figs.(5-8) where the original ACCOME equilibrium points are indicated by black triangles. We define

$$\beta_p \equiv \frac{8\pi^2 p_{avg}}{\mu_0 I^2} \left(\frac{1}{2\pi} \oint_a dl_p \right)^2 \quad 1(a)$$

$$q_* \equiv \frac{2\pi R_0 B_0}{\mu_0 I} \left(\frac{1}{2\pi} \oint_a \frac{dl_p}{R} \right)^2 \quad 1(b)$$

so that in these diagrams, lines of constant β_N are straight with varying slope, and lines of constant β are $\beta_p \propto q_*^2$ parabolas.

The first three ACCOME equilibria, and those derived from them by scaling, have the same normalized pressure profile and rather close values of $p(0)/p_{avg}=(2.7 - 3.0)$, $q_{min}/q_0=(0.6 - 0.8)$, $q_{min}/q_*(0.4 - 0.6)$, and $\rho_{min}=(0.7 - 0.8)$. For the second and third cases (corresponding to typical limiter-defined plasmas), where q_a is a well defined quantity, q_{min}/q_a is also approximately the same and is close to 0.5. Therefore a comparison of the stability results for these three cases provides a good picture of the geometrical (elongation and triangularity) effects at constant pressure and current profiles. The fourth case has the same geometrical parameters as the first one, but more peaked pressure profile, $p(0)/p_{avg}=4.5$ and smaller negative shear area, $\rho_{min}=0.6$. Thus a comparison between the first and fourth cases sheds light on the profile effects at constant geometry.

Our stability results are summarized in Figs.(5-8) where we display the marginal stability boundary for the $n=1$ external mode in the $\beta_p - q_*$ planes spanned by scaling

the aforementioned four ACCOME equilibria. As discussed earlier, we consider only the region with $q_{\min} > 2$ where the $n=1$ mode is the limiting instability and where attractive, completely stable configurations with high beta and high bootstrap current fraction are found. The marginal stability curves show a characteristic structure correlated with integer values of q_{\min} , with optimal β_N limits at q_{\min} somewhat higher than the integers. For the limiter-type elliptical and circular cases, a secondary structure associated with integer values of q_a is apparent. We have shown the $n=2$ stability curve in one case, in order to verify that this mode is no worse than the $n=1$, and that the adopted profiles do not give rise to "infernal-mode-like" behavior which would be characterized by approximately constant values of β_p at the minima of the $n=1$ and $n=2$ curves.

In the geometry scan, comparing figures 5 through 7, we observe a significant increase in the optimal β_N (from 2.2 to 3.7) between the circular or elliptical shapes and the triangular one. In addition, the elongated (elliptical or triangular) cases have an approximate factor of 2 increase in the normalized current I/aB relative to the circular case, for the same optimal values of q . These two effects combined make up for an approximate factor of 3.5 increase in the β limit for the D-shape relative to the circle. Also, the D-shape reaches its optimal beta at a significantly higher value of β_p which results in a higher bootstrap fraction. The relevant figures of merit from this geometry scan are given in Table I.

In the profile scan, comparing figures 5 and 8, we observe that the broader profile is favored, even if we adopt β_* , the root average of the squared pressure, as the more fusion relevant figure of merit. Table II summarizes this result.

We have also investigated the stabilizing effect of a perfectly conducting wall on the external modes. For this we have considered the shaped configurations with broad profiles of Figs. 1 and 5. A continuous, conformally shaped wall around the plasma at a distance $0.3a$ from its boundary allows an increase of the optimal β_N from 3.7 to 5.3, the limiting instability being now the $n=3$ mode.

As a final comment, it is important to note that, in seeking the optimal values of the fusion relevant parameters β or β_* , it is desirable to maximize not only the normalized β_N but also the normalized current I/aB at which the maximum stable β_N occurs. Maximizing

the plasma current should also be important for confinement reasons. This consideration is especially pertinent to the reversed shear configurations, for which the critical β_N exhibits a significant oscillatory variation with the current, as shown in Figs. 5-8. Although the optimal value of β_N occurs at a fairly invariant value of q_{\min} (in the range of 2.1 – 2.3), the corresponding values of I/aB vary significantly with the geometrical and profile parameters of the plasma equilibrium, as evidenced by the scales on the horizontal axes of Figs. 5-8. In addition to the higher β_N , the higher allowed values of I/aB contribute to the superior performance of the highly shaped geometry relative to the circular, and the broad profiles relative to the narrow ones.

IV. Summary and Conclusions

A combined 0-D power balance, current profile control calculation, and ideal MHD stability code has been used to assess negative magnetic shear modes of operation in Alcator C-Mod. These studies indicate it should be possible to establish highly shaped, reversed shear equilibria in C-Mod near the β -limit, with modest levels of current drive and heating power. Furthermore, these discharges can be sustained for time scales beyond the characteristic current diffusion time ($\tau_{L/R} \lesssim 3 - 4$ sec.).

It was found that plasma betas up to 2.60% ($B_0 = 4.0$ T) could be achieved for 4-6 MW of total heating power, assuming an H-mode enhancement factor of 2.5. At these parameters up to 800 kA of current could be sustained non-inductively using 3 MW of off-axis LHCD power and (0.15 - 0.5) MW of central FWCD power. The remaining current was provided by the bootstrap effect with bootstrap current fractions in excess of 0.70. These equilibria were characterized by negative central shear with $q_{\min} > 2$, $q_0 > q_{\min}$, $q_{\min}/q_* \simeq (0.4 - 0.6)$, and $\rho_{\min} \simeq (0.6 - 0.7)$.

The effects of plasma shaping (elongation and triangularity) on the ideal MHD stability of these C-Mod equilibria were investigated in detail. Without a conducting shell, the $n=1$ external mode was found to be the limiting instability in all the configurations that were studied. The critical β_N for $n=1$ stability was $\beta_{N\max} \simeq 3.7$ in the highly shaped C-Mod cross-section with $\kappa_x \simeq 1.80$, $\delta_x \simeq 0.70$, and a broad pressure profile characterized by $p(0)/p_{\text{avg}} = (2.7 - 3.0)$. The critical β_N was observed to decrease to about 2.2 in the elliptical ($\kappa_x \simeq 1.80$, $\delta_x \simeq 0.1$) and circular ($\kappa_x \simeq 1.0$, $\delta_x \simeq 0$) configurations. Also,

the elongated equilibria (elliptical and triangular) had about twice the normalized current (I/aB) as did the circular equilibrium. The improvement in ideal stability due to plasma shaping and the increase in current combined to give an approximate factor of 3.5 increase in the β -limit for the highly shaped configuration relative to the circular case. Also a higher bootstrap current fraction is achieved in the triangular configuration because the equilibrium reaches its critical β at a significantly higher value of β_p . With a conducting shell at a distance $0.3a$ from the plasma edge, the beta limit for highly shaped configurations with broad profiles increases to $\beta_{Nmax} \simeq 5.3$ and is determined by the $n=3$ external mode.

Finally we examined the effect of profile peaking on the $n=1$ stability limit for the highly shaped configuration and found a decrease in β_{Nmax} from 3.7 to 3.2, as $p(0)/p_{avg}$ increased from 2.9 to 4.5.

Table I. Summary of geometry scan results at $A=2.9$ and $p(0)/p_{\text{avg}} \simeq 3$

κ	δ	β_N^{opt}	β^{opt}	β_*^{opt}
1.0	0	2.2	1.1%	1.5%
1.8	0	2.1	2.4%	3.2%
1.8	0.7	3.7	3.7%	5.0%

Table II. Summary of profile scan results at $A=2.9$, $\kappa=1.8$ and $\delta=0.7$

p_0/p_{avg}	ρ_{min}	β_N^{opt}	β^{opt}	β_*^{opt}
2.8	0.7	3.7	3.7%	5.0%
4.5	0.6	3.2	2.4%	3.8%

References

- [1] R.J. Goldston et al., in Proceedings of the 20th European Conference on Controlled Fusion and Plasma Physics, Lisbon, 1993 (European Physical Society, Lisbon, Portugal, 1993) p. I-319.
- [2] C. Kessel, J. Manickam, G. Rewoldt, and W.M. Tang, Phys. Rev. Lett **72**, (1994) 1212.
- [3] A.D. Turnbull, T.S. Taylor, Y.R. Lin-Liu, and H. St. John, Phys. Rev. Lett. **74**, (1995) 718.
- [4] F.M. Levinton, M.C. Zarnstorff, S.H. Batha et al., Phys. Rev. Lett. **75**, (1995) 4417.
- [5] E.J. Strait, L.L. Lao, M.E. Mauel et al., Phys. Rev. Lett **75**, (1995) 4421.
- [6] "ITER Physics Design Guidelines: 1989," N.A. Uckan and ITER Physics Group, (IAEA, Vienna, 1990) ITER Documentation Series No. 10.
- [7] D.R. Mikkelson and C.E. Singer, Nuclear Technology/Fusion **4**, (1983) 237.
- [8] S.P. Hirshman, Phys. Fluids **31**, (1988) 3150.
- [9] G.R. Harris, "Comparisons of Different Bootstrap Current Expressions," Rep. EUR-CEA-FC-1436, Département de Recherches sur la Fusion Contrôlée, Centre d'études de Cadarache, Saint-Paul-lez-Durance (1991).
- [10] P.T. Bonoli, M. Porkolab, J.J. Ramos, D.T. Blackfield, R.S. Devoto, M.E. Fenstermacher, Nuclear Fusion **30**, (1990) 533.
- [11] R.S. Devoto, D.T. Blackfield, M.E. Fenstermacher, P.T. Bonoli, M. Porkolab, G. Tinios, Nuclear Fusion **32**, 773 (1992).
- [12] M. Azumi, G. Kurita, T. Matsuura, T. Takeda, Y. Tanaka, T. Tsunematsu, in Computing Methods in Applied Sciences and Engineering, North-Holland, Amsterdam (1980) 335.
- [13] K. Tani, M. Azumi, and R.S. Devoto, Journal of Computational Physics **98**, (1992) 332.
- [14] P.T. Bonoli and R.C. Englade, Physics of Fluids **29**, (1986) 2937.

- [15] P.T. Bonoli, R.C. Englade, M. Porkolab, and M.E. Fenstermacher, in Proceedings of the Europhysics Topical Conference on Radiofrequency Heating and Current Drive of Fusion Devices, eds. C. Gormezano, P.U. Lamalle, R.R. Weynants, (Brussels, 1992), Vol. 16E p. 169.
- [16] J. Delucia, S.C. Jardin, A.M.M. Todd, Journal of Computational Physics **37** (1980) 183.
- [17] R.C. Grimm, R.L. Dewar, and J. Manickam, Journal of Computational Physics **49**, (1983) 94.
- [18] C.F.F. Karney and N.J. Fisch, Physics of Fluids **28**, (1985) 116.
- [19] M. Brambilla and T. Krücken, Nuclear Fusion **28**, (1988) 1813.
- [20] D.A. Ehst and C.F.F. Karney, Nuclear Fusion **31**, (1991) 1933.
- [21] S.P. Hirshman and D.J. Sigmar, Nuclear Fusion **21**, (1981) 1079.
- [22] I.H. Hutchinson, R. Boivin, F. Bombarda et al., Physics of Plasmas **1**, (1994) 1511.
- [23] H. P. Furth, P. H. Rutherford and H. Selberg, Phys. Fluids **16**, (1973) 1054.
- [24] R. J. Hastie and J. B. Taylor, Nuclear Fusion **21**, (1981) 187.
- [25] J. Manickam, N. Pomphrey and A. M. M. Todd, Nuclear Fusion **27**, (1987) 1461.

Figure Captions

- Figure 1: ACCOME results for current profile control in highly shaped plasma configuration with broad pressure profile ($\kappa_\chi = 1.77$ and $\delta_\chi = 0.71$). (a) Flux contours. (b) Current densities (MA/m²) versus normalized square root toroidal flux (ρ). (c) Safety factor versus ρ .
- Figure 2: ACCOME results for current profile control in elliptical plasma configuration with broad pressure profile ($\kappa_\chi = 1.86$ and $\delta_\chi = 0.10$). (a) Flux contours. (b) Current densities (MA/m²) versus normalized square root toroidal flux (ρ). (c) Safety factor versus ρ .
- Figure 3: ACCOME results for current profile control in circular plasma configuration with broad pressure profile ($\kappa_\chi = 1.00$ and $\delta_\chi = 0.07$). (a) Flux contours. (b) Current densities (MA/m²) versus normalized square root toroidal flux (ρ). (c) Safety factor versus ρ .
- Figure 4: ACCOME results for current profile control in highly shaped plasma configuration with peaked pressure profile ($\kappa_\chi = 1.78$ and $\delta_\chi = 0.71$). (a) Current densities (MA/m²) versus normalized square root toroidal flux (ρ). (b) Safety factor versus ρ .
- Figure 5: Stability limit against the n=1 external mode in the absence of conducting walls, in an $\varepsilon\beta_p$ vs. q_* space spanned by scaling the triangular ACCOME equilibrium with broad profiles depicted in Fig. 1. The location of this original equilibrium is indicated by the black triangle and the stable domain is below the curve. Mode resonant values of q_{\min} along the marginal stability curve are indicated by arrows.
- Figure 6: Stability diagram analogous to that of Fig. 5, for elliptical equilibria with broad profiles after the configuration of Fig. 2. Here we have indicated the mode resonant values of both q_{\min} and q_a .
- Figure 7: Stability diagram analogous to those of Figs. 5 and 6, for circular equilibria with broad profiles after the configuration of Fig. 3. Here the thresholds for n=1 and n=2 external modes are shown, and resonant values of both q_{\min} and q_a are indicated by arrows.

Figure 8: Stability diagram analogous to those of Figs. 5 through 7, for triangular equilibria with narrow profiles after the configuration of Fig. 4.

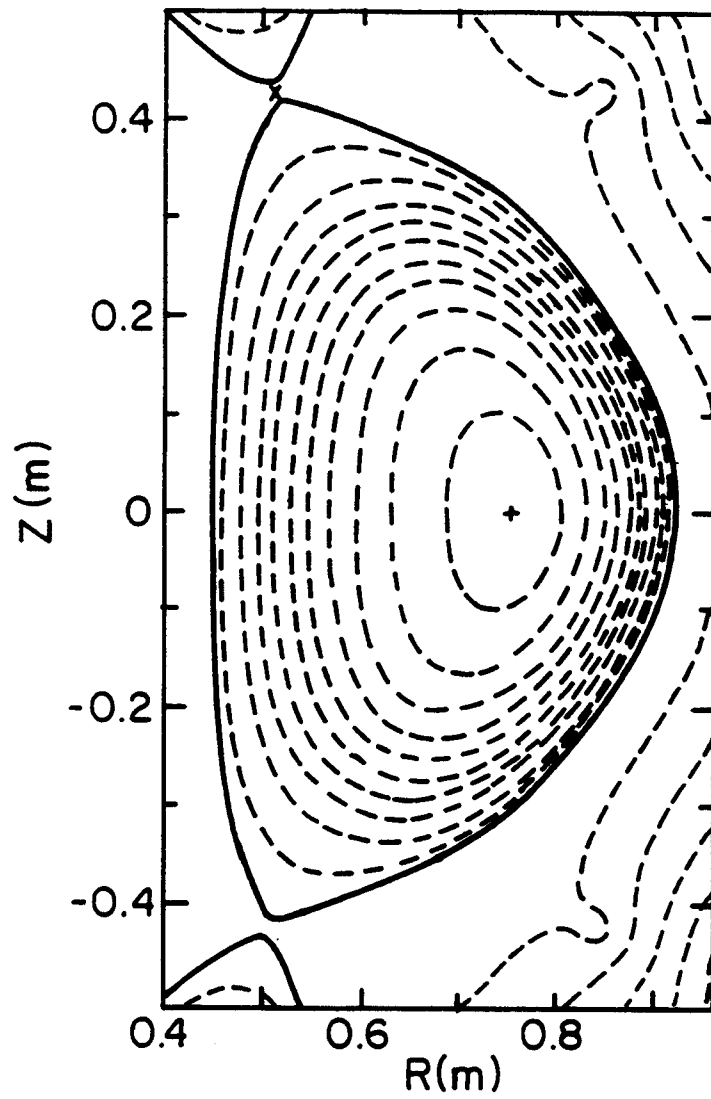


Fig. 1(a)

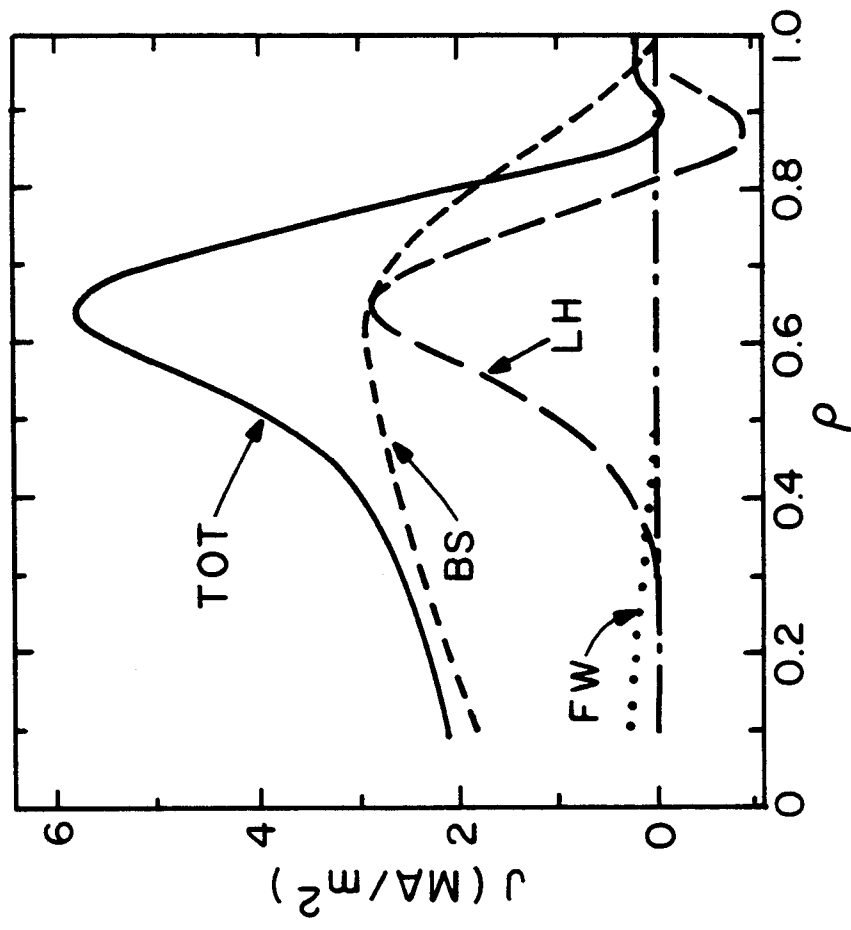


Fig. 1(b)

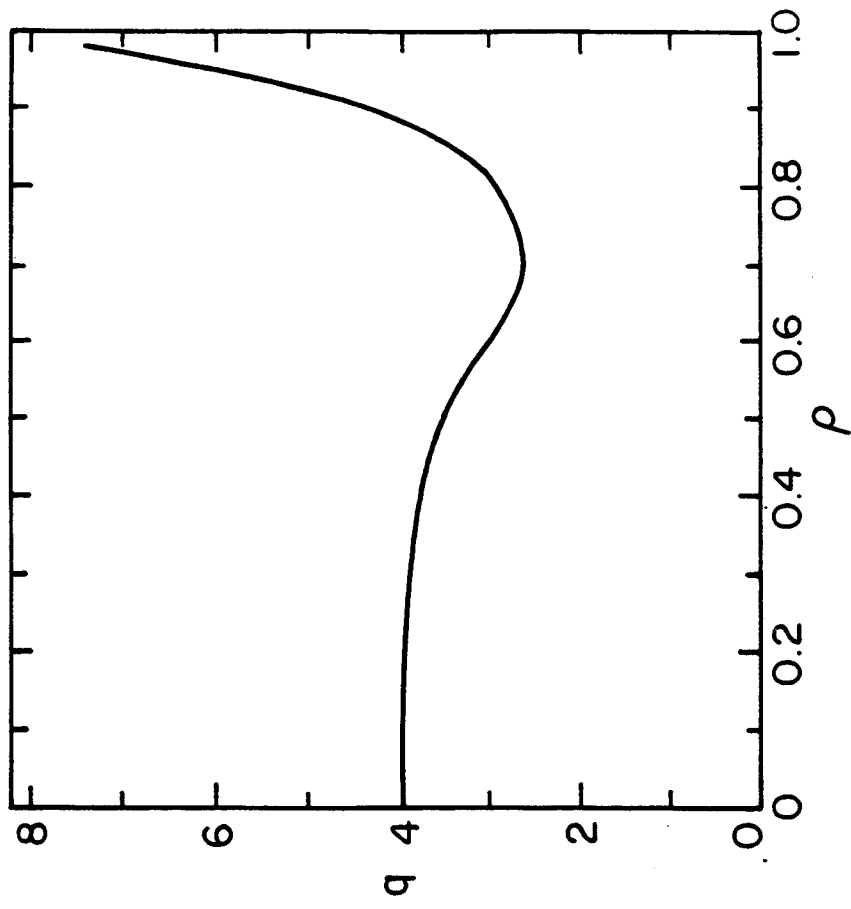


Fig. 1(c)

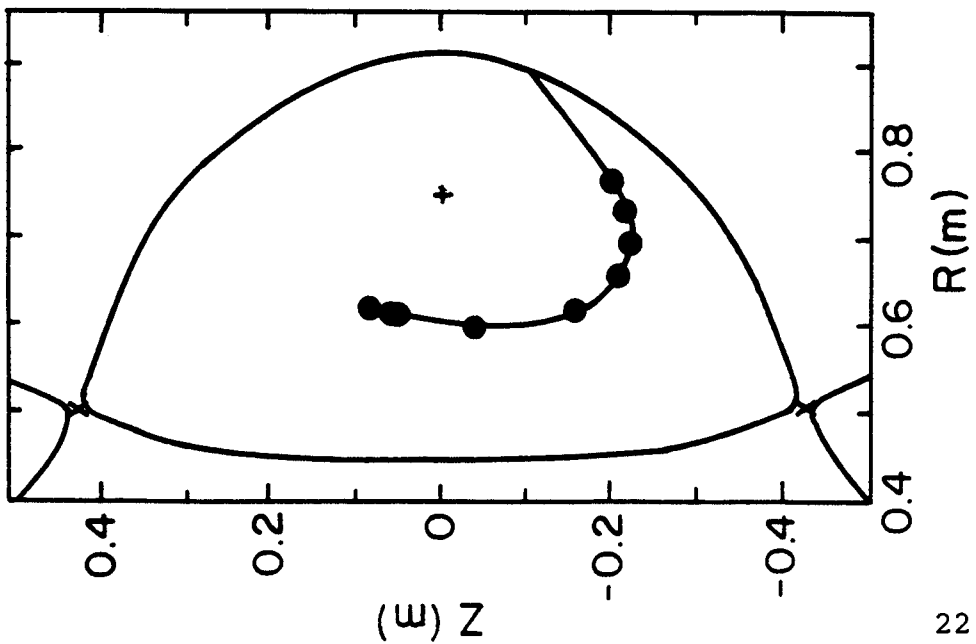
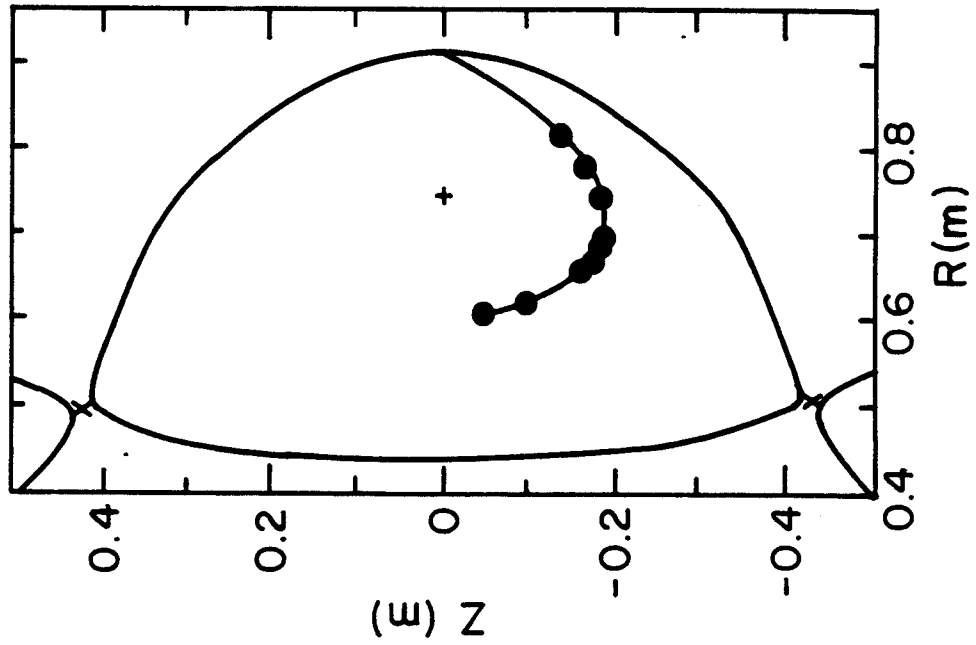
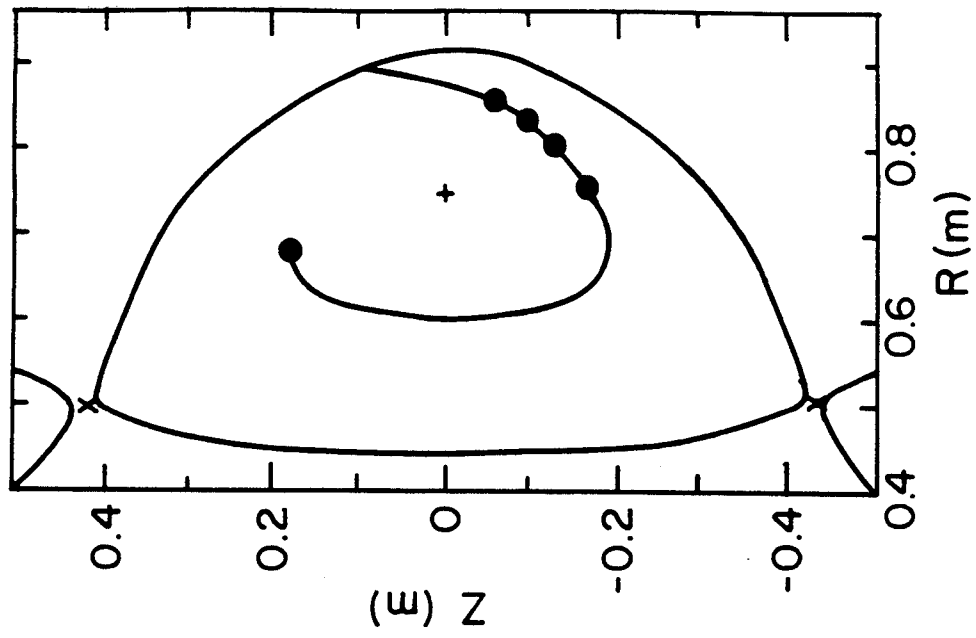


Fig. 1 (d)

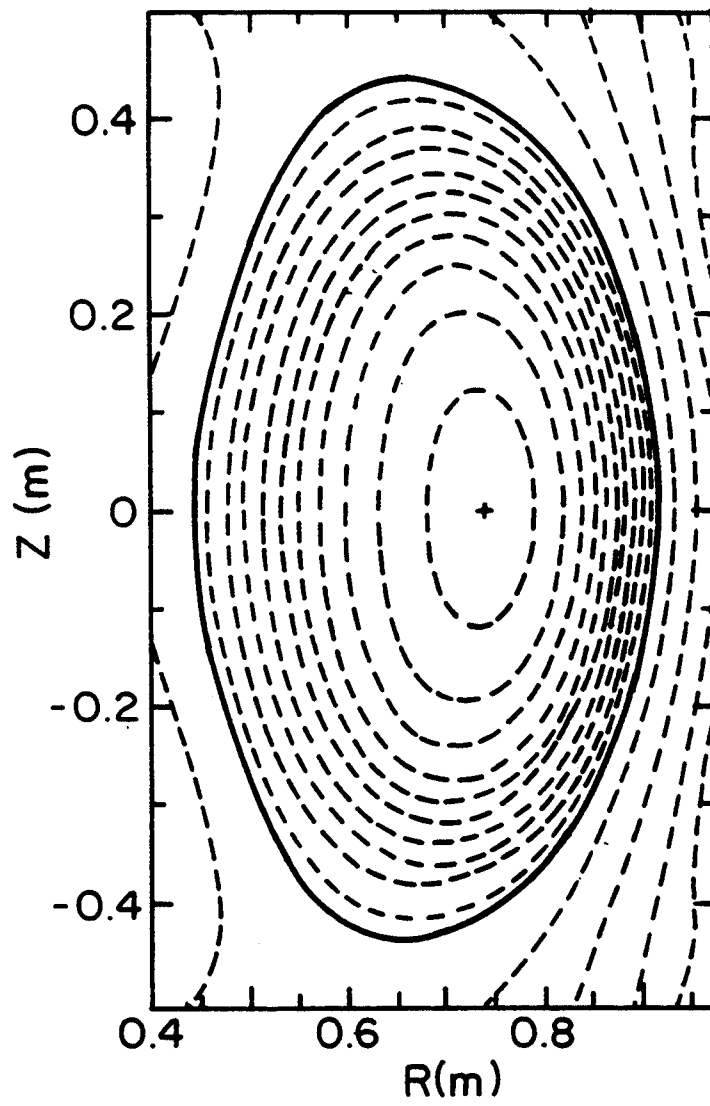


Fig. 2(a)

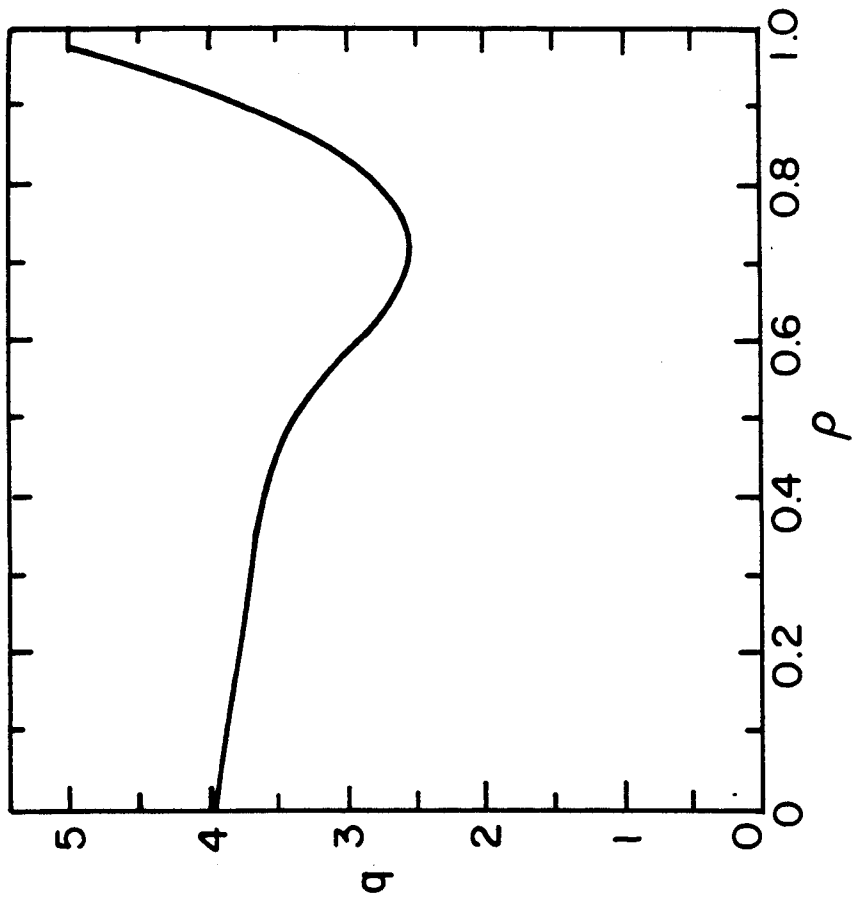


Fig. 2(c)

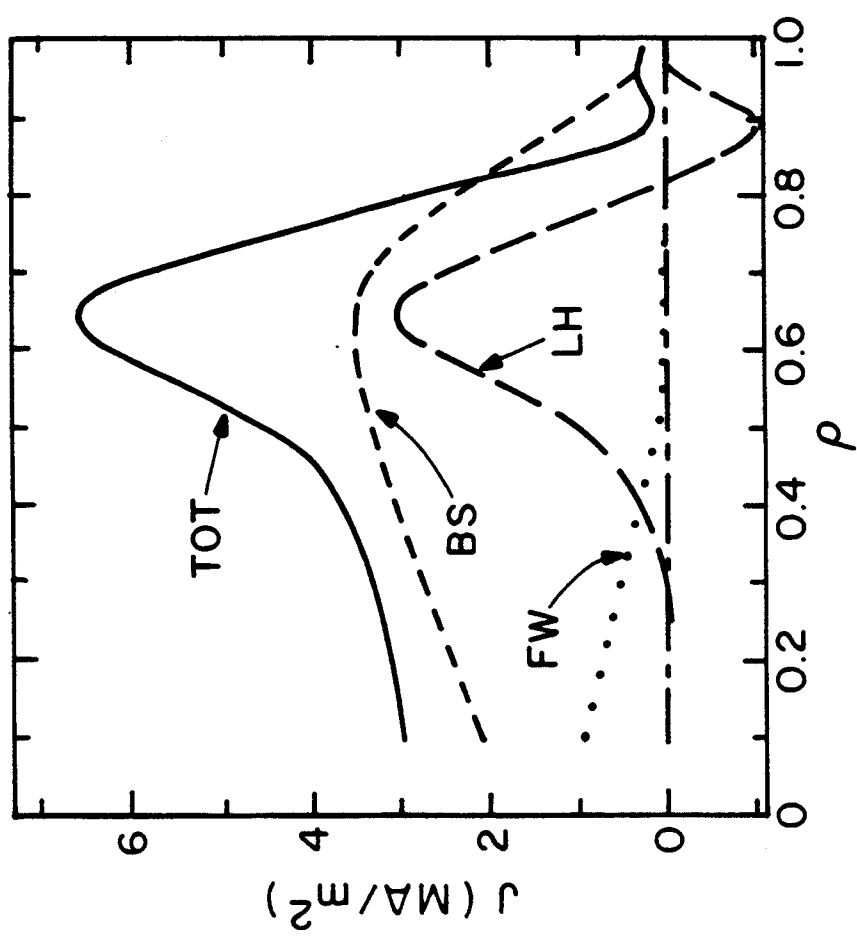


Fig. 2(b)

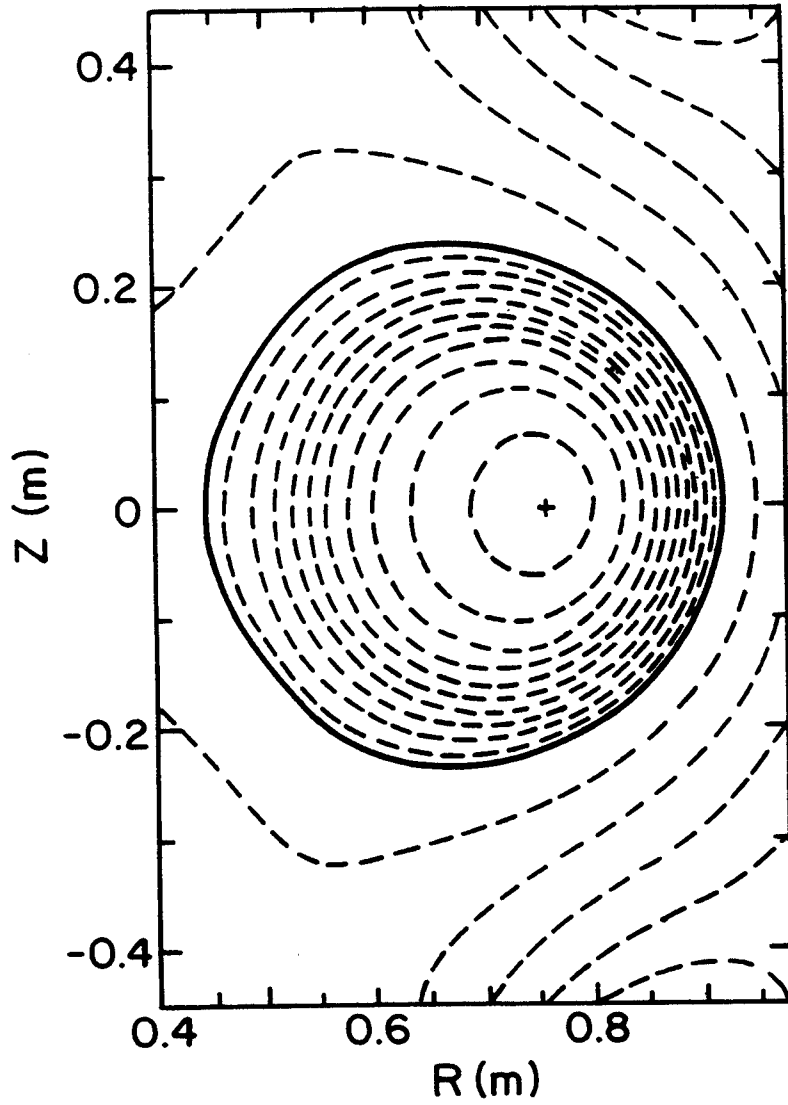


Fig. 3 (a)

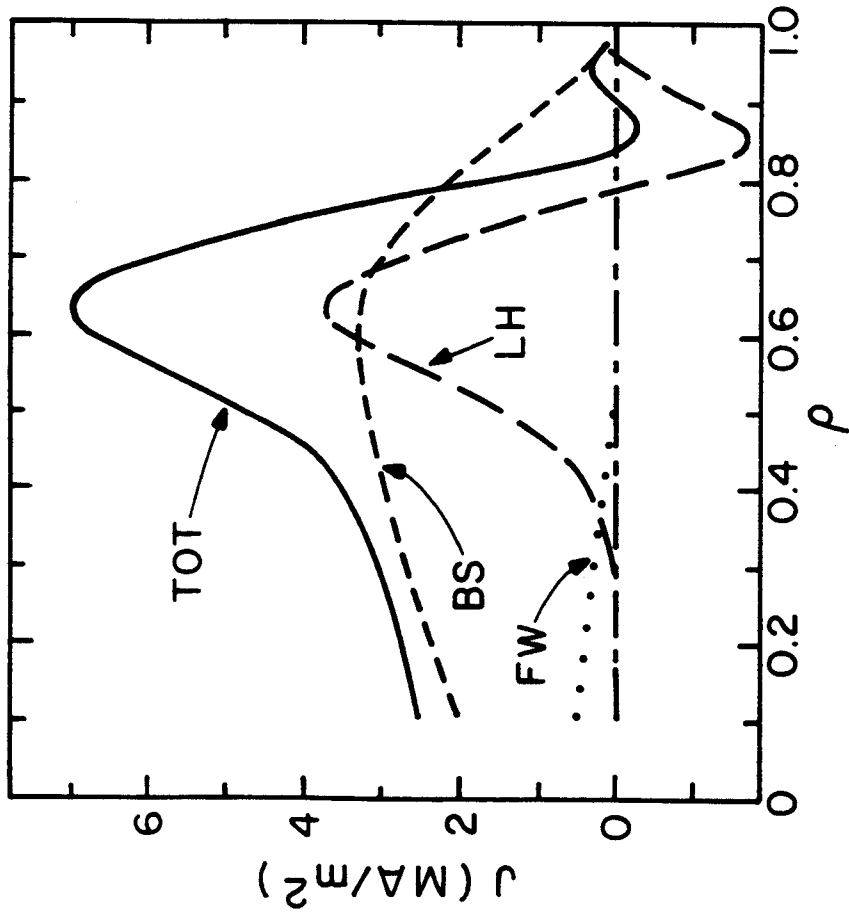


Fig. 3(b)

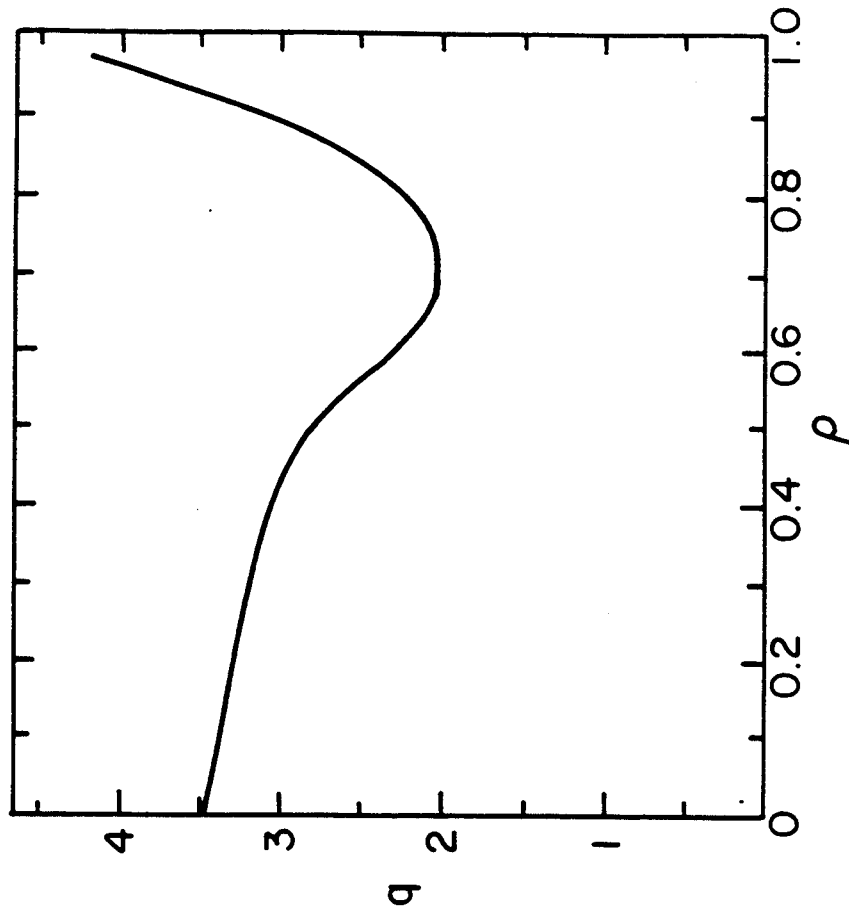


Fig. 3(c)

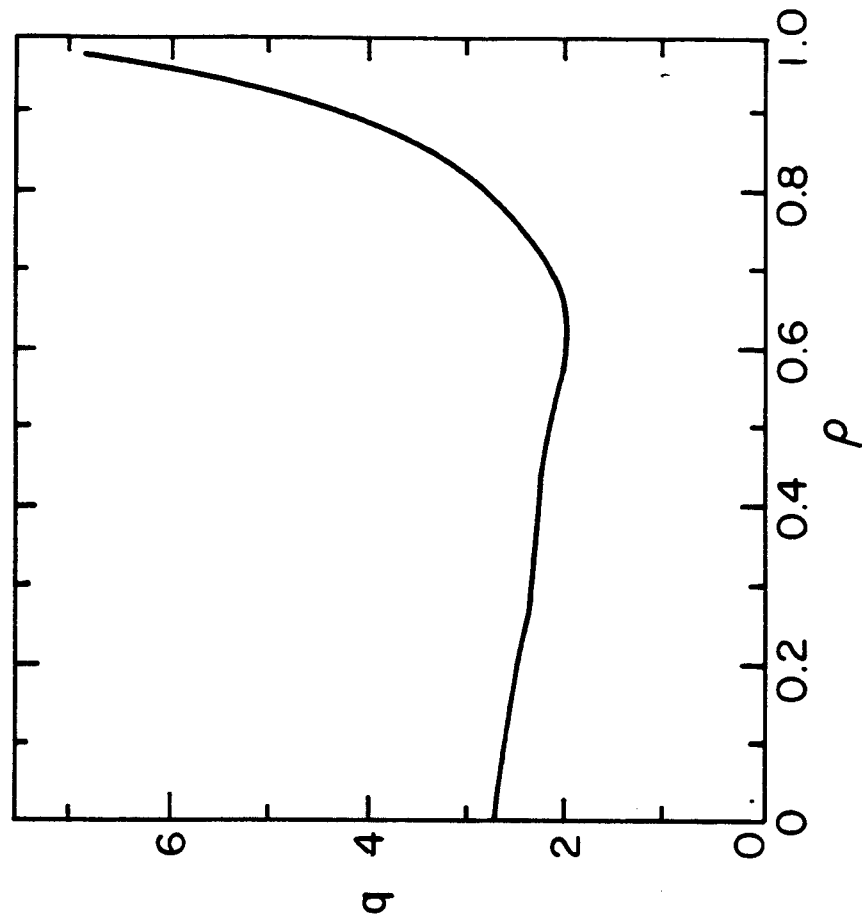


Fig. 4(b)

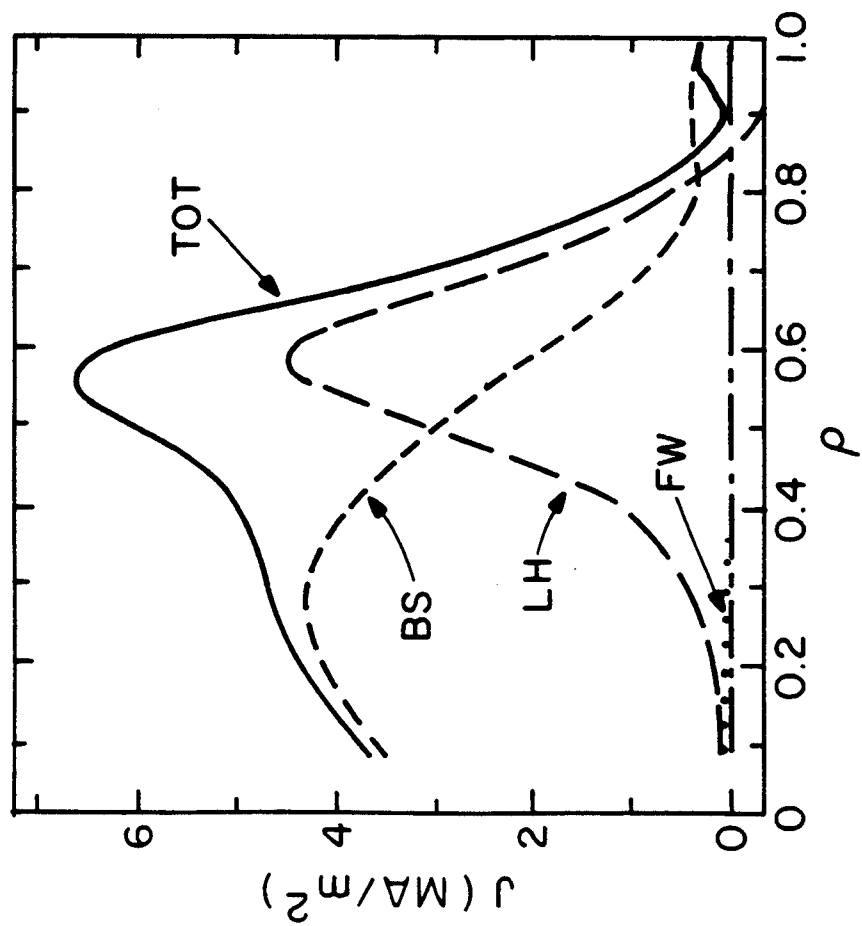


Fig. 4(a)

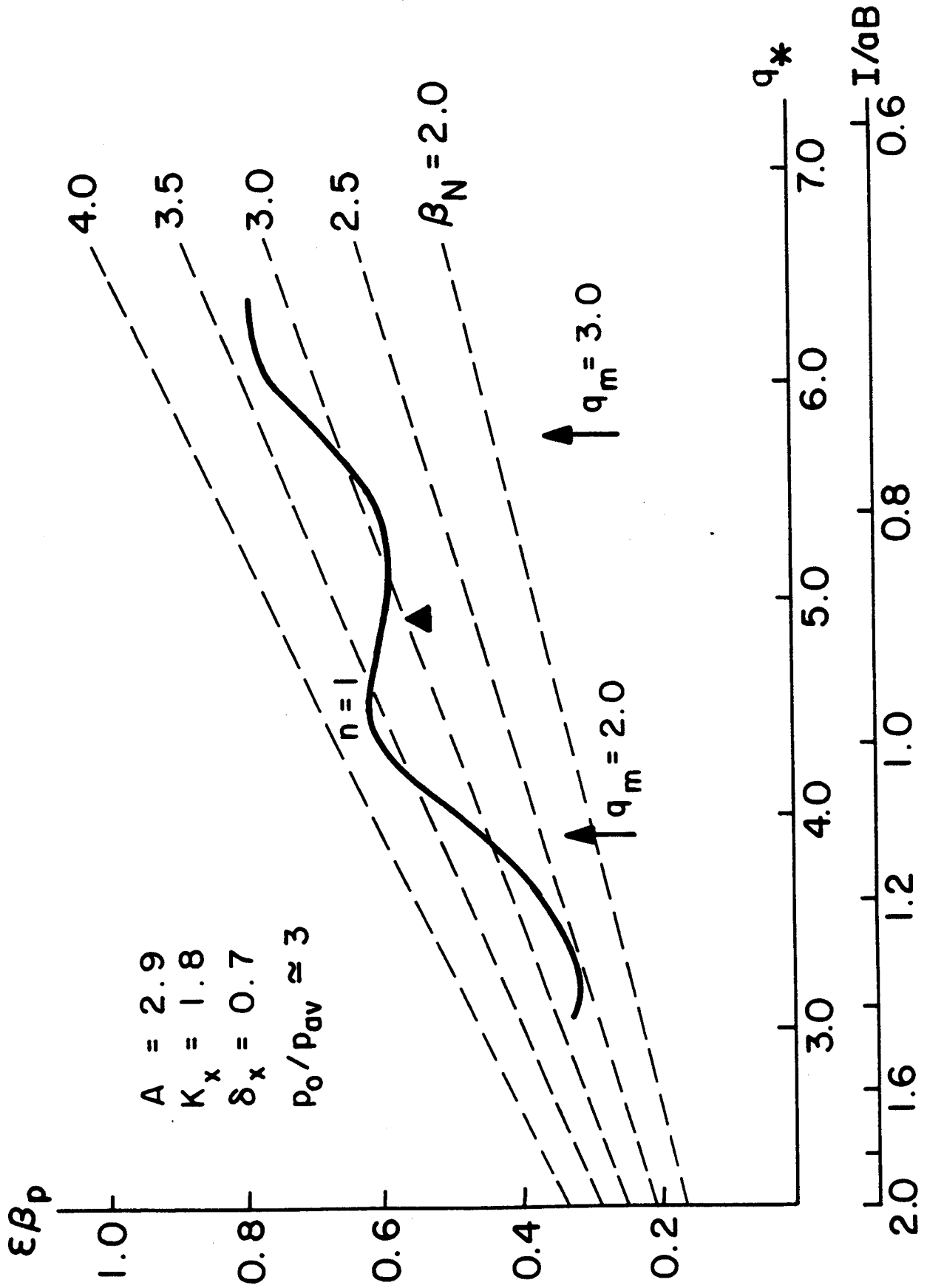


Fig. 5

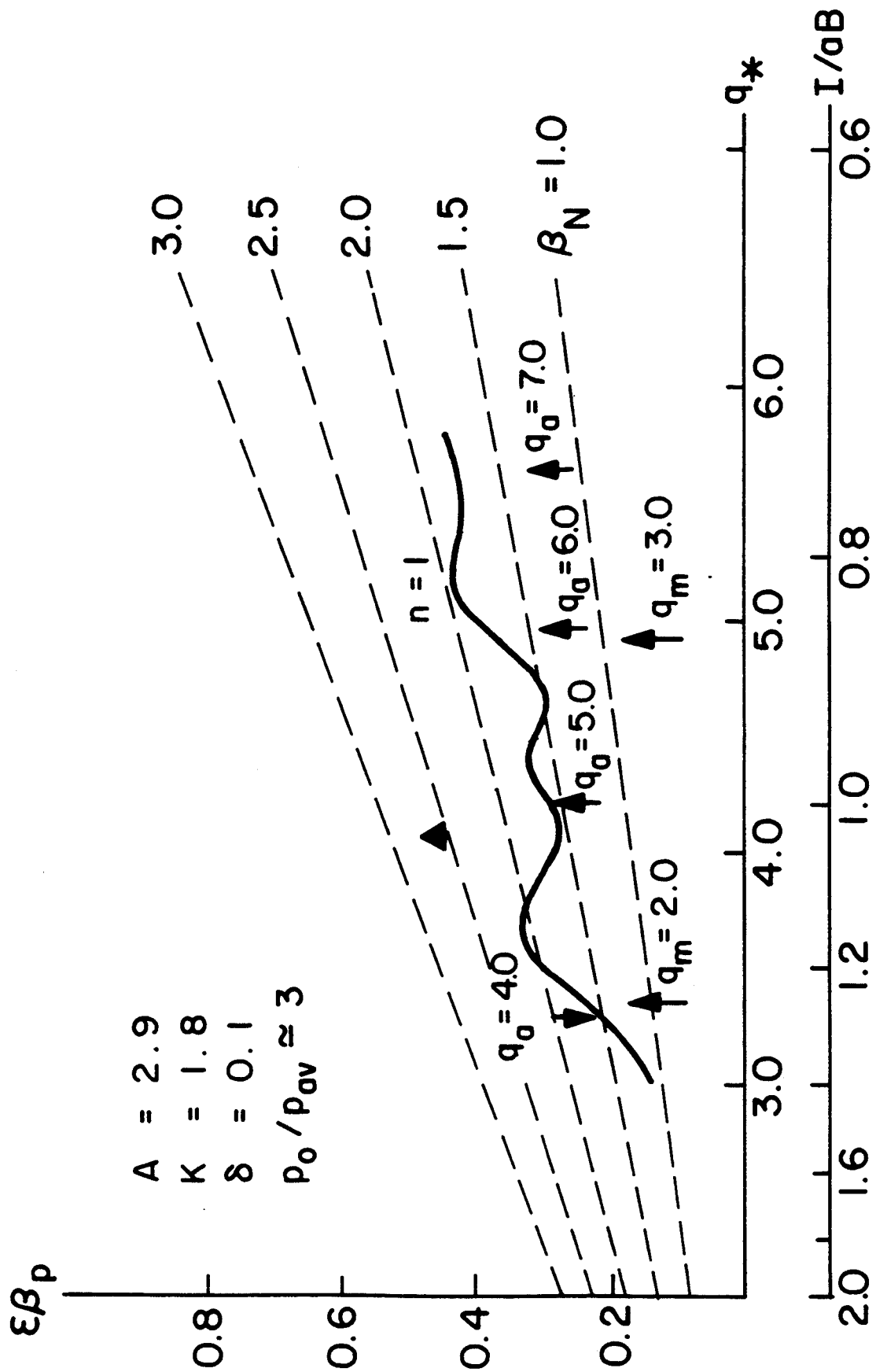


Fig. 6

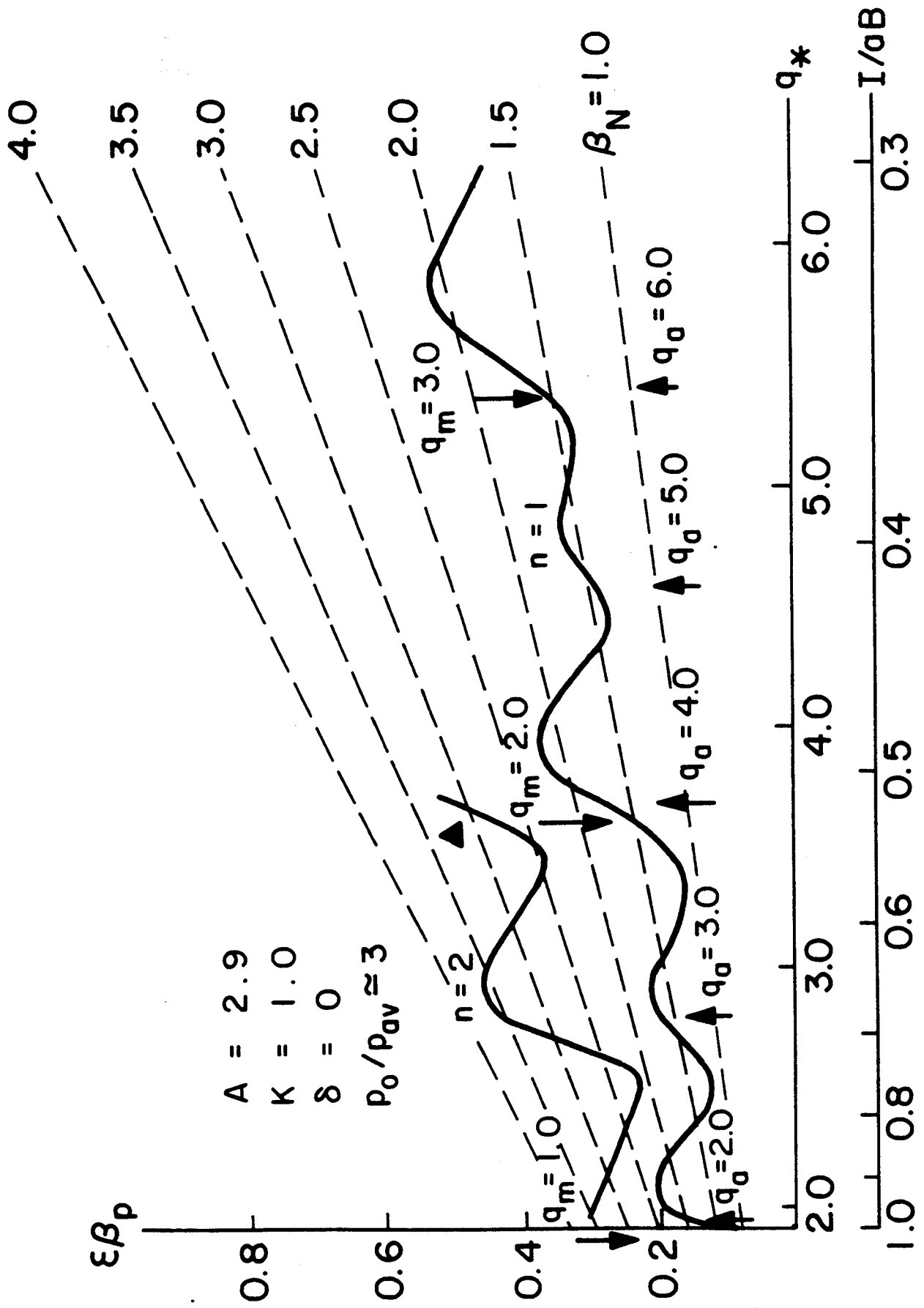


Fig. 7

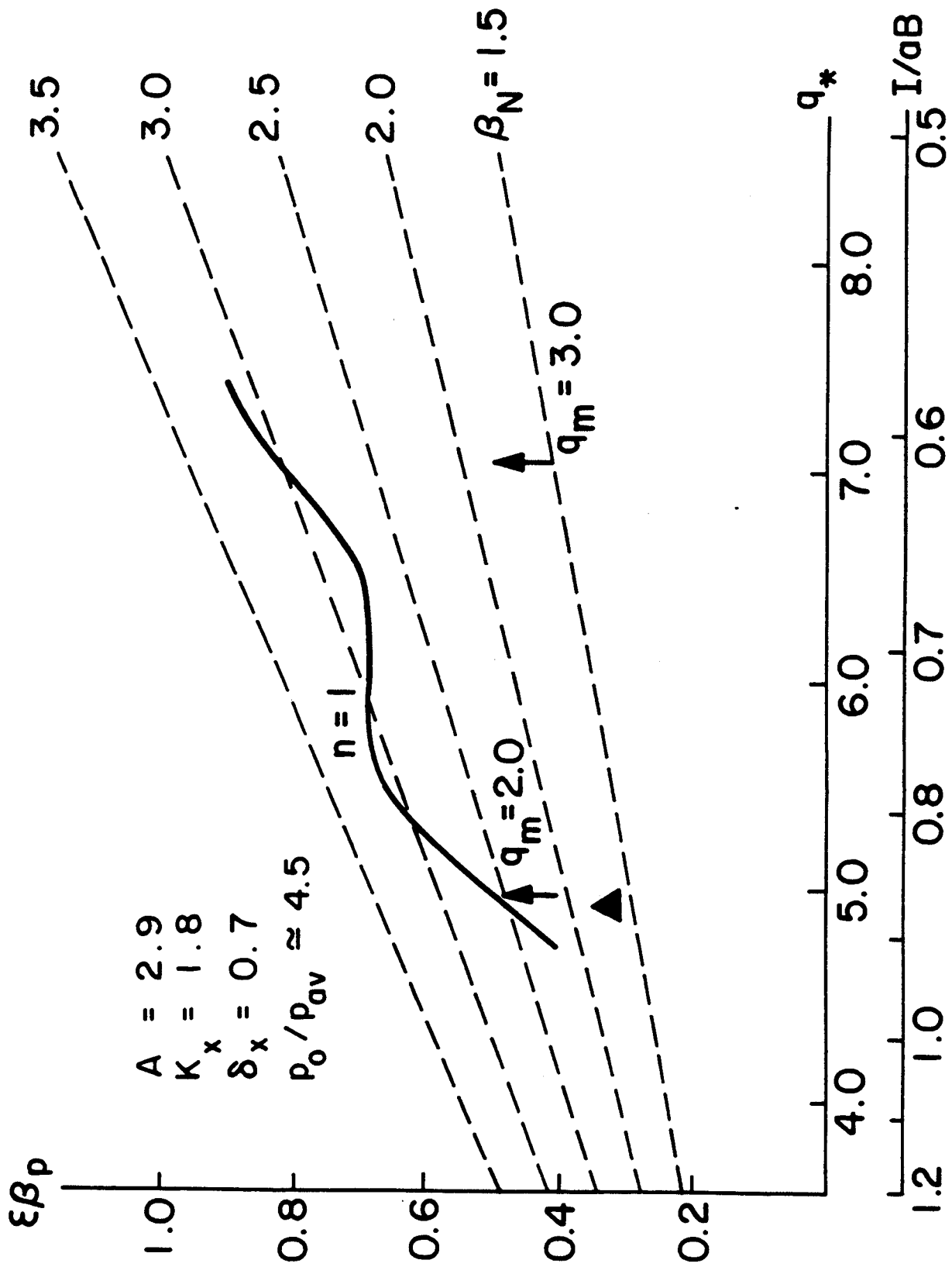


Fig. 8